

# Load Modeling of Electric Bus Charging Station from Data Obtained Through Phasor Measurement Units

Ricardo Isaza – Ruget<sup>1</sup>, Cristhian Perilla<sup>2</sup> and Javier Rosero-García<sup>3\*</sup>

<sup>1,2,3</sup>Universidad Nacional de Colombia; risazar@unal.edu.co<sup>1</sup>, caperillag@unal.edu.co<sup>2</sup>, jaroserog@unal.edu.co<sup>3</sup>

\*Correspondence: Javier Rosero-García; jaroserog@unal.edu.co

**ABSTRACT-** While the increased adoption of electric vehicles (EVs) is a promising alternative to reduce CO<sub>2</sub> emissions, it creates new challenges for the power grid due to increased energy demand and power quality (PQ) issues. These impacts vary depending on several factors such as the level of EV adoption, charging technology, network voltage level, charging patterns, charging station location, battery condition, and driving habits. Analyzing these impacts and developing solutions, such as characterizing the demand curve for charging stations and understanding EV charging patterns, is crucial to ensure a sustainable transition to an electrified EV future. A study using the ZIP load model that represents voltage dependence by combining constant impedance (“Z”), constant current (“I”), constant power (“P”) components, and phasor measurement units (PMUs) demonstrates the effectiveness of EV demand characterization. The importance of this aspect for grid stability and charging management is highlighted.

**Keywords:** load model, electric vehicle, minimum mean squared error (List three to ten pertinent keywords specific to the article, yet reasonably common within the subject discipline).

## ARTICLE INFORMATION

**Author(s):** Ricardo Isaza – Ruget, Cristhian Perilla and Javier Rosero-García;

**Received:** 28/08/2024; **Accepted:** 16/10/2024; **Published:** 25/10/2024;

**e-ISSN:** 2347-470X;

**Paper Id:** IJEER 2808-20;

**Citation:** 10.37391/ijeer.120409

**Webpage-link:**

<https://ijeer.forexjournal.co.in/archive/volume-12/ijeer-120409.html>



**Publisher's Note:** FOREX Publication stays neutral with regard to Jurisdictional claims in Published maps and institutional affiliations.

## 1. INTRODUCTION

The Earth is currently experiencing a constant increase in temperature due to the accumulation of greenhouse gases (GHG). Consequently, solutions are sought to reduce them. One of the major contributors of emissions is the transport sector [1]. Electric vehicles that use electric batteries to power electric motors are presented as an alternative to replace vehicles that use internal combustion engines which use fossil fuels that increase GHG emissions [2]. To promote the use of electric vehicles, some European countries have resorted to subsidies to purchase and lower taxes on these vehicles [3]. EVs are a promising alternative for reducing CO<sub>2</sub> emissions, but their large-scale adoption creates challenges for the electric grid. Increased power demand can lead to PQ problems such as harmonics, undervoltage, phase unbalance, and increased energy loss [4], [5], [6]. These impacts vary depending on several factors including the level of EV adoption, charging technology, voltage level of the network, charging patterns, charging station location, battery condition, and driving habits [7]. It is crucial to deeply analyze these impacts and develop

solutions to ensure a sustainable transition to an electrified future with EVs [8]. Considering these factors affecting the power grid, there is the case of electric chargers to power the batteries of EVs. Due to their power electronics components, they have different dynamic behaviours compared to traditional grid-connected loads. This requires characterization to determine the demand curve of the charging stations; with this characterization, it is possible to determine how the load affects the network in terms of stability and when there are disturbances in the network to formulate programs for load control, load limiting, and voltage and frequency regulation [9]. This characterization also allows for the possibility of demand management. It is important to understand the charging patterns of EVs because their charging behaviour is variable and depends on many factors [10]. In addition to this, there is the uncertainty of when and where vehicles will be charged and the total energy demand of these vehicles in each area. To address these issues, current research focuses on analysing the impact of charging patterns and model-based control strategies. Therefore, the development of mathematical models of EV charging patterns becomes a key aspect that will allow scientists to perform more realistic studies to forecast energy demand and propose solutions to the problems that may arise [6], [11].

## 2. LOAD MODELING

### 2.1. ZIP Model

This load model can be classified into three types: constant power, constant current, and constant load impedance; this classification depends on the ratio of power and voltage. For a constant load, the dependence of power on voltage is quadratic; for a constant current, it is linear; and for a constant power, it is independent of voltage [12], [13], [14], [15]. This model is represented as follows:

$$P = P_o \left[ a_1 \left( \frac{V}{V_o} \right)^2 + a_2 \left( \frac{V}{V_o} \right) + a_3 \right] \quad (1)$$

$$Q = Q_o \left[ a_4 \left( \frac{V}{V_o} \right)^2 + a_5 \left( \frac{V}{V_o} \right) + a_6 \right] \quad (2)$$

The values  $V_o$ ,  $P_o$ , and  $Q_o$  are the initial conditions of the system to be modeled and the coefficients  $a_1$  to  $a_6$  are model parameters [14],[15].

## 2.2. Exponential model

The exponential model is expressed as a representation of the linear model, but with the voltage-dependent power as an exponential function, as shown in the following equation:

$$P = P_o \left( \frac{V}{V_o} \right)^{np} \quad (3)$$

$$Q = Q_o \left( \frac{V}{V_o} \right)^{nq} \quad (4)$$

The exponential parameters  $np$  and  $nq$  are specific to the model, in which there are different values depending on the type of load describing the voltage dependence of the active and reactive load, respectively [15].

**Table 1.**  $np$  and  $nq$  values for common loads

Load Component	$np$	$nq$
Air-conditioning	0.50	2.50
Heaters	2.00	0.00
Pumps and fans	0.08	1.60
High-load industrial motors	0.05	0.50
Low-load industrial motors	0.10	0.60

If the  $np$  or  $nq$  values are equal to 0.1 or 2, the load model will represent the cases of constant power, constant current, or constant impedance [15], [16].

## 2.3. Frequency model

This model is a parameter that can be included in the previous ones to be frequency-dependent and is represented as follows:

$$[1 + A(f - f_o)] \quad (5)$$

The value  $f_o$  represents the nominal frequency of the system and  $f$  represents the frequency of the element being measured in Hertz; the parameter  $A$  represents the frequency sensitivity of the model [15], [17].

## 2.4. Dynamic exponential model

$$T_p \frac{dP_r}{dt} + P_r = P_o \left( \frac{U}{U_o} \right)^{as} - P_o \left( \frac{U}{U_o} \right)^{a1} \quad (6)$$

$$P_l = P_r + P_o \left( \frac{U}{U_o} \right)^{a1} \quad (7)$$

The  $U_o$  and  $P_o$  values are the voltage and power before a voltage change.  $P_r$  is the active recovery power,  $P_l$  is the total active power,  $T_p$  is the active load recovery time constant,  $as$  is

transient active load-voltage dependence coefficient, and  $as$  is steady state active load-voltage dependence coefficient [18].

## 2.5. Mean Square Error (MSE)

$$MSE = \frac{1}{n} \sum_{i=1}^n (y_i - \tilde{y}_i)^2 \quad (8)$$

The root mean square error is used in regression and prediction model evaluation mode by measuring the differences between the values predicted by the model and the values measured. This value is calculated from the phasor measurement unit data and the data predicted from the ZIP model [19].

## 2.6. Optimization algorithm

An optimization algorithm is used in which the values  $Z$ ,  $I$ ,  $P$ , voltage, and power measured at the charging station by the phasor measurement unit are taken as input. From these data, a cost function is performed that takes the parameters of model [12] and calculates the MSE between the active power and the active power predicted by the model. With these data, the model can be optimized by minimizing the cost function that is defined, in which the values  $Z$ ,  $I$ , and  $P$  that minimize the value of the MSE are found.

## 2.7. Rate of Change of Frequency (ROCOF)

In today's power systems, the Rate of Change of Frequency (ROCOF) is defined as the first time derivative of frequency; it is an essential component in several applications, including Wide Area Monitoring, Protection, and Control (WAMPAC). These applications range from load shedding to electrical island detection and distributed generation control [20].

PMUs have the ability to perform ROCOF measurements quickly and with high responsiveness, meeting the rigorous IEEE C.37.118.1 accuracy standards [2]. This involves providing updated ROCOF estimates with reporting rates reaching tens of frames per second (fps), keeping the uncertainty at reduced levels of 0.01 Hz/s in stable conditions, 6 Hz/s in the presence of harmonic distortions, and 3 Hz/s in dynamic situations. In addition, PMUs enable a distributed measurement infrastructure that facilitates synchronous monitoring of voltage and current phasors at various points in the network [21].

ROCOF measurement becomes fundamental in the control of the electrical network, especially in the activation of the Load Disconnection process. This is because ROCOF values vary according to the particularities of the electrical network, with contingency events generating the highest values [2]. During a contingency, such as a power grid failure, the ROCOF may increase significantly, indicating the need to disconnect certain loads to maintain system stability. In addition, negative ROCOF values indicate load imbalances that require immediate adjustments to avoid problems in the network. However, during the process of restoring the network after a contingency, the

variation of ROCOF values depends on the restoration actions, which makes it difficult to accurately predict these values [21]. It is essential to note that a persistent positive value of ROCOF does not necessarily guarantee the safe capacity of the power grid to support an increased load [22]. The safety and reliability of the power grid are critical; to achieve this, it is necessary to apply appropriate filters to the ROCOF estimates. These filters help reduce abrupt transitions and long-term oscillations in the system frequency after contingencies, contributing to maintaining stability. It is also important to note that the ROCOF filtering process leads to a 500 ms delay in the ROCOF relay interventions, which may influence the predictive capability of this parameter, since there is a time lag before the necessary measures are taken to maintain network stability [22]. Taylor Fourier signal compression based model (csTFM), enhanced interpolated DFT (eIpDFT), and iterative interpolated DFT (iIpDFT) are approaches to estimate the ROCOF in non-stationary signals [18]. csTFM uses a second-order Taylor expansion and a dynamic signal model to estimate the ROCOF along with other fundamental parameters, while eIpDFT and iIpDFT are based on a static signal model and use interpolation techniques to improve frequency resolution. It is important to note that static approaches calculate the ROCOF as an incremental ratio with a processing delay equal to the reporting period, while dynamic approaches relate the ROCOF to instantaneous frequency variations, but are more susceptible to noise and interference [20].

For reliability regulation purposes, the ROCOF calculation method proposed by the North American Electric Reliability Corporation (NERC) involves calculating the frequency change in the first 0.5 seconds after a frequency perturbation [22].

$$RoCoF = \frac{f - f_{0.5}}{0.5} \quad (9)$$

### 3. FIELD TEST

The growing demand for electric transportation has driven the need to develop accurate models to predict and manage electric load. In this work, in order to analyse the charging behaviour in an electric transport system, a Siemens UC Charge electric bus charging system was equipped with a phasor measurement unit under the scheme shown *figure 1*. With this equipment, it was possible to obtain high-resolution data, which will be used to evaluate the ability of the ZIP load model to accurately represent the charging dynamics in this type of system. PMUs provide measurements of voltages and currents in phasor form with the addition of positioning and time data through a GPS device that is incorporated in the measuring equipment [21]. For this test, Power side micro phasor measurement units (uPMU) were used, which collect data through current transformers (CT) with 200 amps to 333 millivolts ratio and voltage probes to the charging station; this charging station is energized at 440 volts. The EV charging station is used for public transport vehicle charging, in which the charging stations deliver power sequentially to three dispensers.

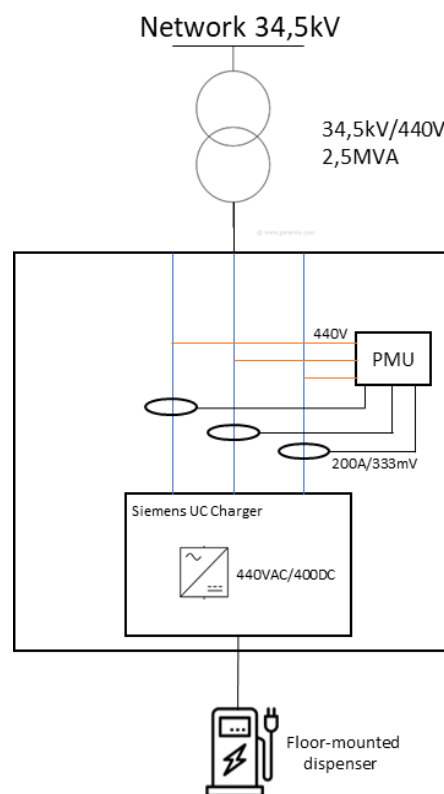


**Figure 1.** Measurement scheme

Measurements made with the uPMU record voltages, currents, active/reactive power, and frequency in phasor form. These data were recorded in a monthly measurement and the behaviour of the charging system on weekdays and weekends was separated, as shown in *figure 1*, in order to use these data in the ZIP model to determine the behaviour of the model in these two types of demand curves.

*Figure 2* shows the result of the demand behaviour during the week of the charging station; it is demonstrated that it is not in service in a range from 4:00 AM to 7:00 PM.

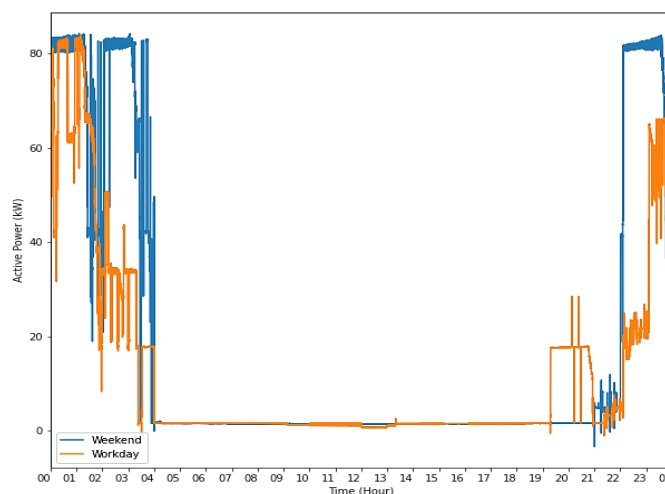


**Figure 2.** Load behavior during the week

In order to validate the ZIP model under controlled conditions, a test field equipped with a configurable load bank was implemented, as shown in *Figure 3*. This bank, composed of resistive and inductive elements, made it possible to simulate a wide range of loads. Variable voltage profiles were applied, which included variations from 0 volts up to a 120, recording the voltage profiles shown in *figure 3*, in order to evaluate the model's ability to adapt to different operating conditions and accurately represent the load behaviour. The same CT configuration was used for the data logging system as for the measurement at the EV charging station.

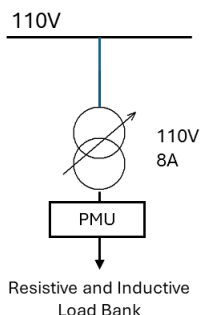


**Figure 3.** Laboratory test system

This load bank relies on five inductors and ten resistors connected in series to increase the load of the network. The following voltage profiles were used in this load bank (see *figure 3*) from the variable transformer connected to the load bank (see *Figure*). This test bank consists of ten resistors and five inductors.

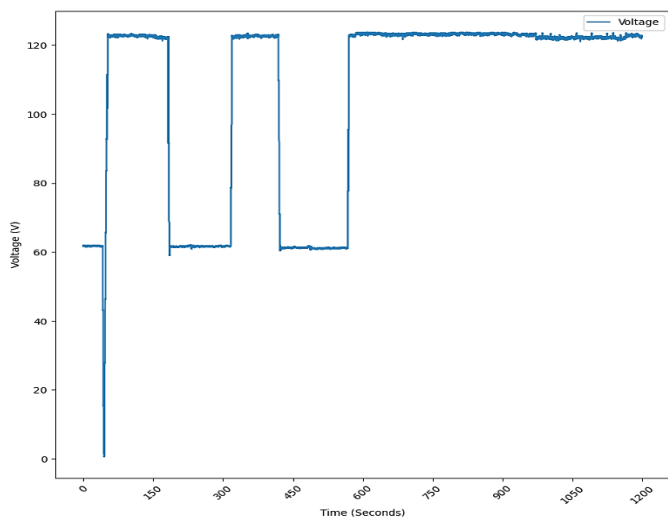


**Figure 4.** Voltage profiles used

Three scenarios were proposed to perform the laboratory tests by applying the voltage profiles shown in *figure 4*. These three scenarios were achieved by disconnecting the inductive and resistive elements that make up the load bank in order to evaluate the load model method in a laboratory setting. In the first scenario, the ten resistors and no inductance were connected. In the second scenario, the ten resistors were left fixed, and the inductances were varied from the minimum

connection to the maximum inductances. In the third scenario, the ten resistors and five inductances were used to obtain the data using the PMU. With this, the proposed algorithm could be implemented.

#### 4. METHODOLOGY

The methodology shown in *figure 5* was used to obtain the values of the ZIP model from the data recorded by the phasor measurement unit, in which these data were used to generate the first parameters of the ZIP model and then the MSE was calculated. With these values, the optimization function could be implemented to reduce the MSE and obtain new parameters to feed the ZIP model in order to find the parameters that fit the MMSE.

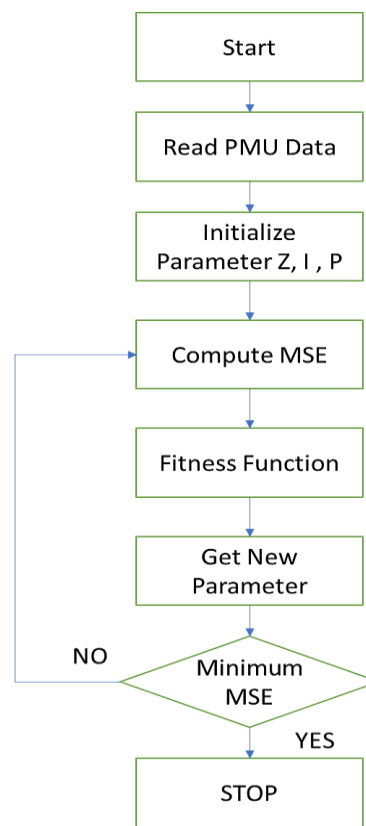


**Figure 5.** Flowchart

The algorithm shown in *figure 5* reads the data obtained from the phasor measurement unit to use the model, cleans the data, and calculates the zero-load probability [24]. Then, it defines the load model function that takes the model parameters Z, I, P, active and reactive power, and voltage as inputs and calculates the total predicted active power [25]. The function that takes the model parameters and the active power, apparent and reactive power data as inputs and calculates the MSE between the real total active power and the total active power predicted by the model is defined [26]. For the optimization process, the minimize function of the SciPy. optimize library [27] is set to minimize the cost function and to find the values of the parameters Z, I, and P that minimize the MSE. From these data, the MSE and the coefficient of determination ( $R^2$ ) are calculated to evaluate the performance of the optimized model.

## 5. ANALYSIS OF RESULTS OF THE ZIP MODEL

The curves shown in *figure 6* obtained with the PMU measurements performed at the electric vehicle charging stations and the laboratory shown in *figure 4* are evaluated by applying the algorithm shown in *figure 5*. This analysis includes time fractions of the curves shown in *figure 6* to evaluate the algorithm model and its behaviour in a smaller amount of data. Additionally, there is the application for the reactive power curve and the behaviour of the algorithm.

By using the proposed methodology, the result is obtained by evaluating the ZIP model for consumption on a business day, shown in *figure 6* in which the values of the ZIP model that result in the MMSE for the input values of the model on a business day shown in *figure 2* are recorded. In this model, shown in *figure 6*, system transients caused by the change of EV charger dispenser are observed. There is a pulse that the model fails to follow, but it manages to follow most of the load curve; an MSE of 2.6% is obtained by using the algorithm proposed. For this model, the input data has a coefficient of determination of 0.99, which is a good input data sample for the model.

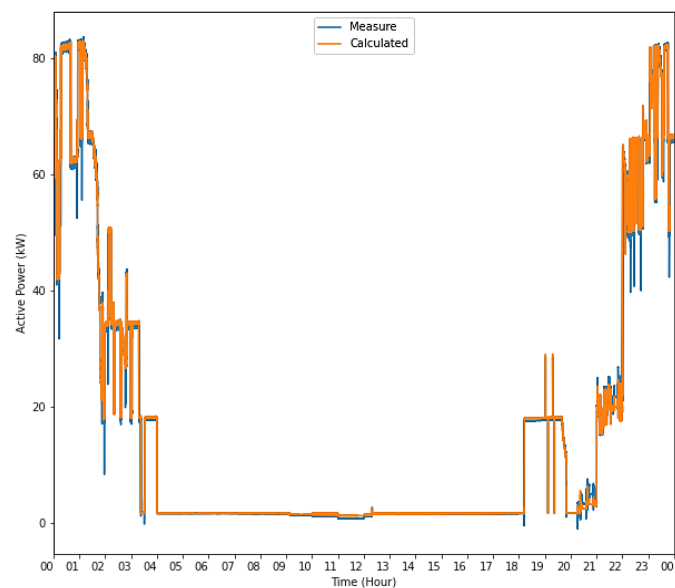


**Figure 6.** Load model for business day demand

Subsequently, the model is evaluated on a smaller sample of the behaviour on a random day during a time window of one hour as shown in *figure 7*, which represents the sequential charging behaviour of the three distributors of the charging station during the charging cycle in this time window. When a transient change occurs, the model generates a pulse and tries to follow the measured curve, but when it does this the model generates a pulse with opposite direction and then stabilizes to follow the measured load curve. The pulses generated by the model obtain an MSE of 2.47% with the input data; these data have a coefficient of determination of 0.99.

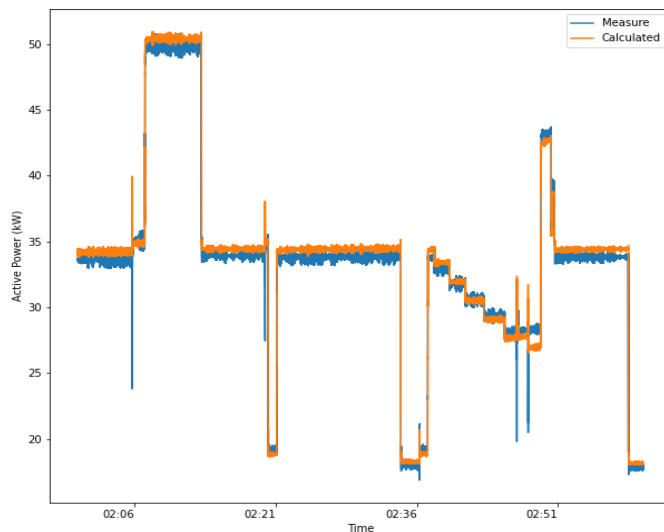


**Figure 7.** Data measured at the charging station by the phasor measuring unit

The measurement shown in *figure 8* analyses a phenomenon that occurs in the EV charging station where there is power delivery. These data show a change of sign of the power factor. More pronounced pulses are obtained, but with a negative sign when delivering energy to the network; this causes new transient phenomena to evaluate the model proposed. When the load model is used for this data, the model does not follow the behaviour in the negative measurements; it generates a pulse trying to follow the same magnitude, but on the positive axis of the active power to continue with the model run. In this case, an MSE of 2.47% is obtained by applying the algorithm to obtain the load model including the pulses that deliver power to the grid.

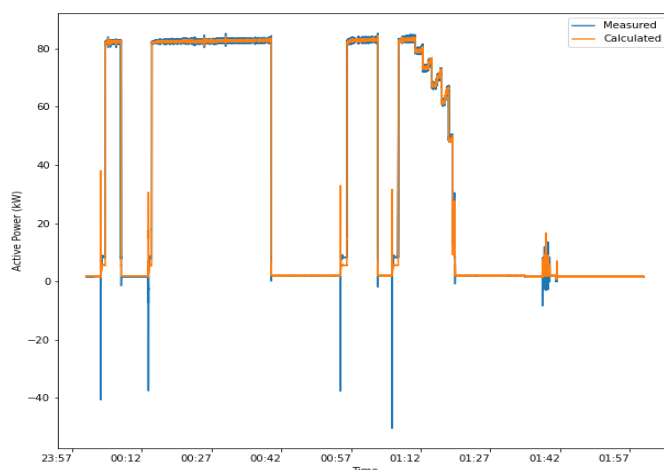


**Figure 8.** ZIP model obtained from active power

The ZIP model is also used for reactive power. The algorithm is evaluated to obtain the load model for the reactive power from the measurements recorded by the PMU as shown in *figure 9*. It is observed that no pulses are found as in the active power measurements shown in *figure 8*. *Figure 9* contains data on the negative axis, but it is not comparable with the amount of data

in the entire measurement. With these data, the load model has a better approximation by applying the proposed algorithm, since it results in an MSE of 2.3% for a data input that has a coefficient of determination of 0.99.

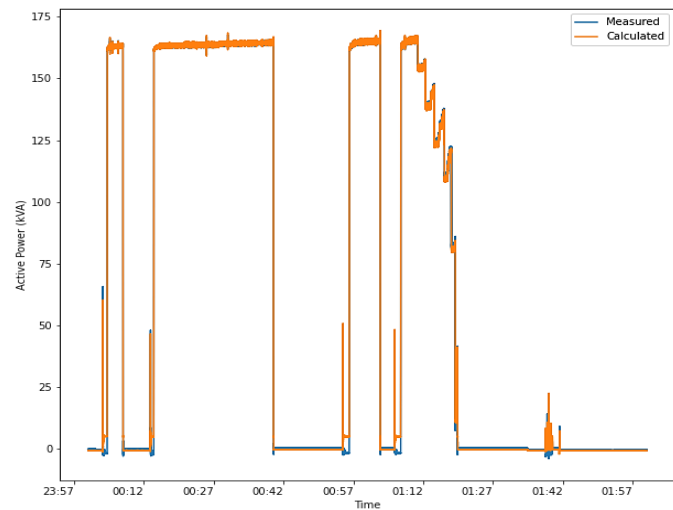


**Figure 9.** ZIP model reactive power

In the laboratory test using a load bank, as shown in *Figure*, there is a larger number of pulses in the data that the model attempts to follow, as shown in *figure 10*. However, when trying to follow it, it generates larger peaks compared to those of the measured data; this generates more error in the obtained model. When evaluating the MSE of the proposed algorithm, a 10% is obtained for a data input with a coefficient of determination of 0.99; this gives a result that shows transient changes. The load model is not a best fit and increases the error with respect to previous data evaluations.

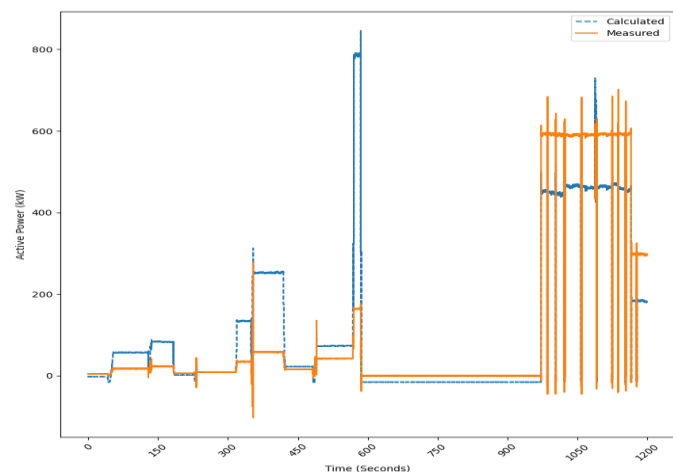


**Figure 10.** Test bank model evaluation

The measurements taken on the test bank show a significant error in the charging model compared to the data obtained at the electric vehicle charging station. From these measurements, the rate of change of frequency (RoCoF) was calculated using the method proposed by NERC [22], which establishes a calculation interval every 500ms.

The analysis revealed a remarkable disturbance between seconds 45 and 46, where the RoCoF reaches a value higher than 200 Hz/s. This unusual behavior, which indicates a considerable disturbance in the system, due to the disconnection of the load from the test bench and bringing the voltage to zero volts as shown in *figure 4* can be seen in *figure 11*, which shows the evolution of both the frequency and RoCoF in that time window.

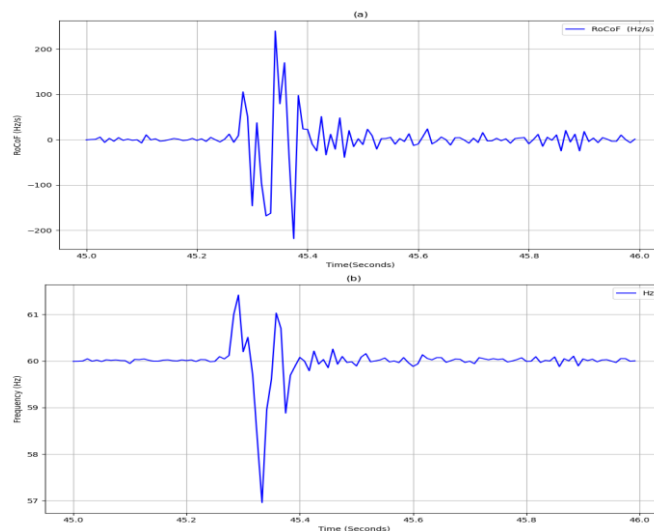


**Figure 11.** (a) Test bank frequency (b) Test bank RoCoF 500ms

In the load model, during the time window in which the disturbance occurs, it is observed that the active power and voltage is equal to zero. However, when trying to follow this behaviour, the load model generates negative values during the disturbance, which significantly increases the error. This behaviour can be seen in *figure 12* where it is shown how the load model diverges from the real values of active power.

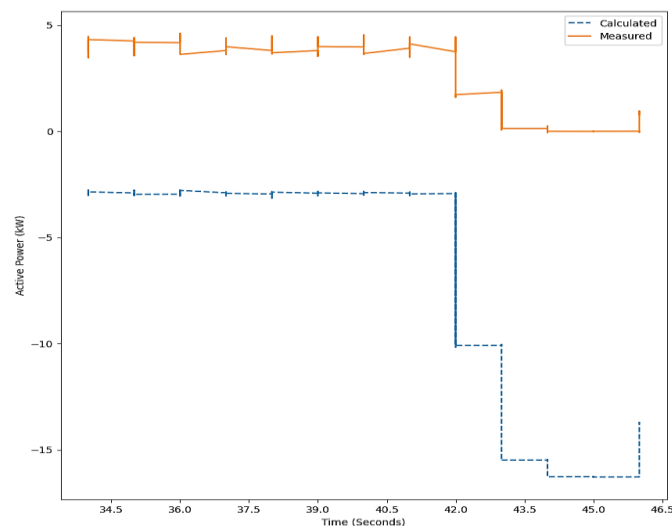


**Figure 12.** Load model and active power applying voltage disturbance

To ensure the reliability of the ZIP Model predictions at an electric vehicle charging station, an evaluation was performed

using statistical tests. The results of the tests as shown in *table 2* ANOVA, Kolmogorov-Smirnov, Jarque-Bera and Durbin-Watson suggest that, while the model captures a significant portion of the variability in the data, there are violations of statistical assumptions that may affect the accuracy of the long-term predictions, and the validity of inferences based on this model.

**Tabla 2. Load model statistical tests**

Prueba	Valor	p-value
ANOVA F-statistic	3.839e-14	-
ANOVA p-value	1.000e+00	1.000
K-S Statistic	2.748e-01	0.000
K-S p-value	0.000e+00	0.000
Jarque-Bera Statistic	5.384e+10	0.000
Jarque-Bera p-value	0.000e+00	0.000
Durbin-Watson Statistic	3.522e-01	-
R-squared	1.000e+00	-

Performing the statistical analysis exhibits a high coefficient of determination ( $R^2=0.9983$ ), suggesting a good fit to the data. However, further analysis of the residuals reveals significant deviations from normality, as indicated by the Kolmogorov-Smirnov and Jarque-Bera tests ( $p < 0.05$  in both). In addition, the Durbin-Watson test (0.3523) points to a strong autocorrelation in the residuals, which questions the independence of the errors. Despite an ANOVA F-value close to zero ( $3.839 \times 10^{-14}$ ), the results of the normality and autocorrelation tests suggest that the assumptions of the linear model are not fully met, limiting the generalizability of the results and the reliability of statistical inferences based on this model.

The ZIP model evaluated from PMU measurements demonstrates its potential to accurately characterize the charging station, although limitations were identified in its ability to model abrupt transients and power factor changes due to the capacitive factor generated by the charging station. Despite these limitations, the model provides a solid basis for power grid planning by being able to perform simulations with this data, extending the capacity of transformers and conductors for large-scale charging systems, demand management and charging station operation optimization. ZIP can be modelled with energy management tools, strategies can be developed to smooth the load curve, reduce operating costs and improve grid stability. In addition, its incorporation into electric vehicle charging management systems can optimize energy utilization and minimize the impact on the grid. Future studies could focus on improving the accuracy of the model for transient events and explore its integration with other more complex load models by integrating Artificial Neural Network Load Modelling for implementation in smart grid design, which would better capture the dynamics of electrical load with more complex behaviour.

## 6. CONCLUSIONS

The model has difficulties in accurately modelling transients caused by abrupt changes in load by the return of energy to the grid in cases of active power evaluation. In the case of reactive power, better accuracy is obtained because there are no peaks generated by the change of the power factor of the same magnitude as found in the active power. The accuracy of the ZIP model depends largely on the quality of the input data. It is recommended that the data be pre-processed to eliminate noise and outliers. Despite the limitations, the ZIP model remains a useful tool for demand estimation in electric vehicle charging systems. In this case, since these data are from the normal operation of the charging station, no voltage changes such as under-voltages or contingencies are made in the data obtained. As a result, the model may not receive enough data to have the best approximation. For this, it is necessary to obtain data on failures, but this contingency phenomenon is unlikely to be found in this voltage level. Additionally, the integration of the ZIP model with energy management systems can be explored to optimize the operation of power grids.

### Acknowledgment

This research was supported by Electrical Machines and Drives (EM&D) from Universidad Nacional de Colombia, Red de cooperación de soluciones energéticas para comunidades, code: 59384.

## REFERENCES

- [1] G. Brückmann and T. Bernauer, "What drives public support for policies to enhance electric vehicle adoption?," *Environmental Research Letters*, vol. 15, no. 9, p. 094002, Sep. 2020, doi: 10.1088/1748-9326/ab90a5.
- [2] F. Alanazi, "Electric Vehicles: Benefits, Challenges, and Potential Solutions for Widespread Adaptation," *Applied Sciences*, vol. 13, no. 10, p. 6016, May 2023, doi: 10.3390/app13106016.
- [3] G. Santos and H. Davies, "Incentives for quick penetration of electric vehicles in five European countries: Perceptions from experts and stakeholders," *Transp Res Part A Policy Pract*, vol. 137, pp. 326–342, Jul. 2020, doi: 10.1016/j.tra.2018.10.034.
- [4] X. Huang, D. Wu, and B. Boulet, "Ensemble Learning for Charging Load Forecasting of Electric Vehicle Charging Stations," in *2020 IEEE Electric Power and Energy Conference (EPEC)*, IEEE, Nov. 2020, pp. 1–5. doi: 10.1109/EPEC48502.2020.9319916.
- [5] L. T. M. Mota and A. A. Mota, "Load modeling at electric power distribution substations using dynamic load parameters estimation," *International Journal of Electrical Power & Energy Systems*, vol. 26, no. 10, pp. 805–811, Dec. 2004, doi: 10.1016/j.ijepes.2004.07.002.
- [6] H.- Rivera et al., "Citation: An Overview of Electric Vehicle Load Modeling Strategies for Grid Integration Studies," 2024, doi: 10.3390/electronics13122259.
- [7] X. Wang, H. J. Kaleybar, M. Brenna, and D. Zaninelli, "Power Quality Indicators of Electric Vehicles in Distribution Grid," in *2022 20th International Conference on Harmonics & Quality of Power (ICHQP)*, IEEE, May 2022, pp. 1–6. doi: 10.1109/ICHQP53011.2022.9808823.
- [8] M. H. Cedillo, H. Sun, J. Jiang, and Y. Cao, "Dynamic pricing and control for EV charging stations with solar generation," *Appl Energy*, vol. 326, p. 119920, Nov. 2022, doi: 10.1016/j.apenergy.2022.119920.

- [9] T. Mannari and H. Hatta, "CIRED workshop on E-mobility and power distribution systems Analysis on the effect of V2G aggregation on distribution network based on traffic simulator," 2022.
- [10] U. Bin Irshad and S. Rafique, "Stochastic Modelling of Electric Vehicle's Charging Behaviour in Parking Lots," in 2020 IEEE Transportation Electrification Conference & Expo (ITEC), IEEE, Jun. 2020, pp. 748–752. doi: 10.1109/ITEC48692.2020.9161566.
- [11] A. Huaman-Rivera, R. Calloquispe-Huallpa, A. C. L. Luna Hernandez, and A. Irizarry-Rivera, "An Overview of Electric Vehicle Load Modeling Strategies for Grid Integration Studies," *Electronics* 2024, Vol. 13, Page 2259, vol. 13, no. 12, p. 2259, Jun. 2024, doi: 10.3390/ELECTRONICS13122259.
- [12] K. Fungyai, N. Sangmeg, A. Pichetjamroen, S. Dechanupaprittha, and N. Somakettarin, "Determination of ZIP Load Model Parameters based on Synchrophasor Data by Genetic Algorithm," 2020 8th International Electrical Engineering Congress, iEECON 2020, Mar. 2020, doi: 10.1109/IEECON48109.2020.229509.
- [13] S. Han et al., "Measurement-based static load modeling using the PMU data installed on the university load," *Journal of Electrical Engineering and Technology*, vol. 7, no. 5, pp. 653–658, 2012, doi: 10.5370/JEET.2012.7.5.653.
- [14] M. Leinakse, Estimation and Conversion of Static Load Models of Aggregated Transmission System Loads.
- [15] I. R. Navarro, "Dynamic Load Models for Power Systems Estimation of Time-Varying Parameters During Normal Operation." [Online]. Available: <http://www.iea.lth.se>
- [16] M. Leinakse, Estimation and Conversion of Static Load Models of Aggregated Transmission System Loads.
- [17] A. Arif, Z. Wang, J. Wang, B. Mather, H. Bashualdo, and D. Zhao, "Load Modeling—A Review," *IEEE Trans Smart Grid*, vol. 9, no. 6, pp. 5986–5999, Nov. 2018, doi: 10.1109/TSG.2017.2700436.
- [18] "Front Matter," in *Variable Generation, Flexible Demand*, Elsevier, 2021, p. iii. doi: 10.1016/b978-0-12-823810-3.01001-3.
- [19] K. M. Ramachandran and C. P. Tsokos, *Mathematical statistics with applications*. Academic Press, 2009.
- [20] G. Frigo, A. Derviskadic, Y. Zuo, and M. Paolone, "PMU-Based ROCOF Measurements: Uncertainty Limits and Metrological Significance in Power System Applications," *IEEE Trans Instrum Meas*, vol. 68, no. 10, pp. 3810–3822, Oct. 2019, doi: 10.1109/TIM.2019.2907756.
- [21] A. Derviskadic, Y. Zuo, G. Frigo, and M. Paolone, "Under Frequency Load Shedding based on PMU Estimates of Frequency and ROCOF," in 2018 IEEE PES Innovative Smart Grid Technologies Conference Europe (ISGT-Europe), IEEE, Oct. 2018, pp. 1–6. doi: 10.1109/ISGTEurope.2018.8571481.
- [22] S. You et al., "Calculate Center-of-Inertia Frequency and System RoCoF Using PMU Data," in 2021 IEEE Power & Energy Society General Meeting (PESGM), IEEE, Jul. 2021, pp. 1–5. doi: 10.1109/PESGM46819.2021.9638108.
- [23] D. Tzelepis, E. Tsotsopoulou, Q. Hong, V. Terzija, and C. Booth, "Measuring technologies for future power grids," *Encyclopedia of Electrical and Electronic Power Engineering: Volumes 1-3*, vol. 2, pp. 310–319, Jan. 2023, doi: 10.1016/B978-0-12-821204-2.00147-1.
- [24] J. Reback et al., "pandas-dev/pandas: Pandas 1.0.1," Feb. 2020, doi: 10.5281/ZENODO.3644238.
- [25] J. D. Hunter, "Matplotlib: A 2D Graphics Environment," *Comput Sci Eng*, vol. 9, no. 3, pp. 90–95, 2007, doi: 10.1109/MCSE.2007.55.
- [26] F. Pedregosa FABIANPEDREGOSA et al., "Scikit-learn: Machine Learning in Python Gaël Varoquaux Bertrand Thirion Vincent Dubourg Alexandre Passos PEDREGOSA, VAROQUAUX, GRAMFORT ET AL. Matthieu Perrot," *Journal of Machine Learning Research*, vol. 12, pp. 2825–2830, 2011, Accessed: Oct. 18, 2022. [Online]. Available: <http://scikit-learn.sourceforge.net>.
- [27] P. Virtanen et al., "SciPy 1.0: fundamental algorithms for scientific computing in Python," *Nat Methods*, vol. 17, no. 3, pp. 261–272, Mar. 2020, doi: 10.1038/s41592-019-0686-2. in Python," *Nat Methods*, vol. 17, no. 3, pp. 261–272, Mar. 2020, doi: 10.1038/s41592-019-0686-2.



© 2024 by the Ricardo Isaza – Ruget, Cristhian Perilla and Javier Rosero-García Submitted for possible open access publication under the terms and conditions of the Creative Commons Attribution (CC BY) license (<http://creativecommons.org/licenses/by/4.0/>).